Quantitative Impact of Thermodynamic Property Model Selection on Gas Turbine Performance Prediction

J.-F. P. Pitot de la Beaujardiere[a], H.C. Reuter[b]

Received 09 May 2014, in revised form 25 July 2014 and accepted 13 November 2014

A variety of working fluid thermodynamic property models are applied in gas turbine performance simulations, potentially giving rise to significant discrepancies in performance prediction. Literature indicates that little attention has been paid to assessing the impact of model sophistication on cycle performance prediction, especially for the case of industrial gas turbines. This paper seeks to investigate this impact by quantifying the correlation between several contemporary models in predicting the performance of a single-shaft gas turbine for varying operating conditions. The models considered represent a spectrum of sophistication; ranging from ideal gas models to advanced models that account for real gas and dissociation effects. Rigorous procedures were used to determine gas turbine state point properties, allowing for performance indices to be calculated for variations in ambient temperature, ambient relative humidity, compression ratio and turbine inlet temperature. The results indicate significant deviations in performance predictions, particularly at high compression ratios and turbine inlet temperatures. In a general sense, the study provides a useful resource to researchers engaged in the selection of suitable caloric property models for gas turbine simulator development.

Additional keywords: Thermodynamic properties, gas turbine, performance prediction

Nomenclature

Roman

h	specific enthalpy
M	molar mass
$\dot{n}$	molar flow rate
p	static pressure
$\dot{q}$	specific heat transfer rate
r	pressure ratio
s	specific entropy
T	static temperature
$\dot{w}$	specific power
$\bar{x}$	mixture composition

Greek

Δ	loss/difference
ε	excess air fraction
η	isentropic efficiency
ϕ	relative humidity

Subscripts

1	compressor inlet
2	compressor outlet
3	turbine inlet
4	turbine outlet
a	air
c	compressor
cc	combustion chamber
f	fuel/formation
g	combustion gas
in	input
is	isentropic
m	molar
mix	mixture
net	net
r	reaction
t	turbine
th	thermal

Acronyms

$Prod$	combustion products
$Reac$	combustion reactants

1 Introduction

As improvements continue to be made in the simulation and performance assessment of gas turbine cycles, the accuracy and efficiency of thermodynamic property models used to estimate cycle state point properties are becoming increasingly important. Although the IAPWS-IF97 formulation[1] for the properties of water and steam enjoys widespread usage by industry, literature does not indicate the existence of a predominant state-of-the-art approach for the calculation of the thermodynamic properties of air and combustion gases. As indicated by Bücker *et al.*[2], a variety of models find acceptance in different circles of industry. Models in use include those presented by Baehr and Diederichsen[3], Brandt[4], McBride *et al.*[5], Gordon and McBride[6], in addition to that proposed in ANSI/ASME PTC 4.4 - 1981[7]. Models introduced fairly recently include those proposed by McBride *et al.*[8], Bücker *et al.*[2], Lanzafame and Messina[9], in addition to that proposed in the VDI Guideline 4670[10]. The NIST-JANAF property database[11] is also considered for performance calculations[12]. Consequently, developers of gas turbine simulation programs are faced with a wide range of models from which to choose. Such a

a. University of KwaZulu-Natal, Discipline of Mechanical Engineering, Durban, South Africa. E-mail: pitot@ukzn.ac.za.
b. Stellenbosch University, Department of Mechanical and Mechatronic Engineering, Stellenbosch, South Africa.

choice must ultimately be guided by a trade-off between model complexity and accuracy.

The difficulty of model selection is compounded by the varying degrees of sophistication possessed by the available models. It would appear that most of the models in use are ideal gas models with caloric properties assumed to be dependent on temperature alone. However, at elevated maximum pressures, low ambient temperatures, or for gas mixtures containing high concentrations of water vapour and/or carbon dioxide, real gas effects begin to influence caloric properties significantly. Another complication arises from species dissociation reactions at elevated maximum temperatures, which result in the introduction of intermediate species and appreciable changes to mixture composition. Numerous thermodynamic property models exist that account for these non-ideal effects and the deviations that arise between the non-ideal and ideal gas models in predicting the properties of gas mixtures typical of gas turbine operation have been demonstrated to be significant.[2,9,13,14]

Surprisingly, model correlation assessments pertaining to the prediction of actual gas turbine performance appear very limited. In the context of propulsion applications, the matter has been given attention by Lee *et al.*[15], Gallar *et al.*[16] and Kyprianidis *et al.*[17] to varying degrees of scope and sophistication. Furthermore, the authors of this study were unable to find any literature providing a quantitative evaluation of the correlation between contemporary models in predicting the performance indices associated with shaft-power gas turbines under varying conditions of operation. In particular, what has not been evaluated is the extent to which model sophistication impacts cycle performance predictions. If such impacts are significant, a question that needs to be addressed is: beyond which operating parameter thresholds should non-ideal effects be accounted for in predicting shaft-power gas turbine performance indices? A further aspect that requires assessment is the level of agreement that exists amongst the categories of contemporary models considered. Since thermodynamic property calculations form the backbone of gas turbine cycle analyses, findings of this nature would provide a useful resource to inform the selection of suitable thermodynamic property models for simulation purposes.

The current study seeks to address the above questions through an evaluation of the correlation between a variety of recently-developed and/or commonly used models in predicting the performance of a shaft-power gas turbine. Correlation results were obtained by employing each model to determine state point properties for the rigorous performance analysis of a shaft-power gas turbine subjected to variations in ambient temperature, ambient relative humidity, compression ratio and turbine inlet temperature. In turn, state point data derived from this process were used to calculate predicted performance indices associated with each model. It is important to note that the purpose of the study was to investigate the relative correlation between the models concerned rather than the correlation between performance predictions and actual gas turbine performance data. By comparing the models on an equivalent basis rather than against actual performance data, all extraneous sources of uncertainty were removed from the assessment, allowing the deviation relationships to be assessed in isolation.

2 Methodology

2.1 Models investigated

The models considered in this work were those presented in the works of McBride *et al.*[5], McBride *et al.*[8], and Lanzafame and Messina[9], the VDI Guideline 4760[10] and the scientific formulation proposed by Bücker *et al.*[2], in addition to those found in version two of the NASA-CEA software developed by Gordon and McBride[6], version eight of the NIST REFPROP software developed by Lemmon *et al.*[18], the fourth edition of the NIST-JANAF Thermochemical Tables[11], and the FluidEXL Graphics LibHuFlueGas for Excel® thermophysical property software developed by Kretzschmar *et al.*[19] In the case of the models particular to the VDI Guideline 4760 and the NASA-CEA code, thermodynamic properties were predicted for both fixed and dissociated compositions.

2.2 Gas turbine performance analysis

For the comparative evaluation of gas turbine performance predictions, a rigorous model of a simple shaft-power gas turbine combusting pure methane was employed (Figure 1).

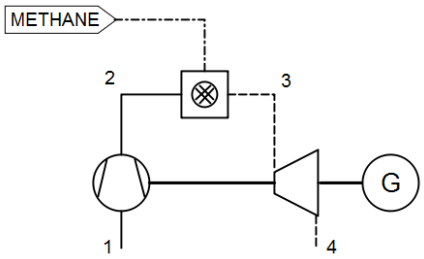

Figure 1: Gas turbine configuration.

The analysis considered the response of five performance indices: compressor specific power input, $\dot{w}_c$, turbine specific power output, $\dot{w}_t$, net specific power output, $\dot{w}_{net}$, specific heat input rate, $\dot{q}_{in}$, and thermal efficiency, η_{th}, to the variation of two ambient parameters: compressor inlet temperature, T_1, and ambient relative humidity, ϕ_1, and two machine parameters: compression ratio, r_c, and turbine inlet temperature, T_3. The nominal values and range of variation of the ambient and machine parameters are reflected in Table 1. Kinetic and potential energy contributions were neglected in the analysis.

The dry air composition considered for the gas turbine performance analysis was a truncated normalized version of that proposed by Gatley *et al.*[20] and is shown on a volumetric basis in Table 2.

The mixture composition, $\bar{x}_a$, of the air working fluid was formulated according to the specified ambient relative humidity and vapor pressure data for water from REFPROP. This allowed the mole fraction of water-to-dry-air to be determined and the normalized composition of the air working fluid to be evaluated. The lower temperature limit associated with thermodynamic data for water in REFPROP is 0.01 °C. Therefore, for ambient temperatures below this limit, only dry air was considered.

Table 1: Nominal values and ranges of variation associated with all ambient and machine parameters.

Param.	Unit	Nom. Value	Lower Limit	Upper Limit
T_1	°C	15	-20	40
p_1	bar	1.013	-	-
ϕ_1	%	60	20	100
r_c	-	15	5	35
η_c	%	0.85	-	-
T_f	°C	25	-	-
η_{cc}	%	99	-	-
Δp_{cc}	%	3	-	-
T_3	°C	1000	800	1300
η_t	%	0.95	-	-

Table 2: Dry air composition on a volumetric basis.

Species	% Composition
Nitrogen	78.0842
Oxygen	20.9441
Argon	0.9332
Carbon Dioxide	0.0385

Fully rigorous calculations were undertaken to determine the total pressure, total temperature, specific enthalpy, h_i, and specific entropy, s_i, at each state point, i, according to the composition of the working fluid involved. When enthalpies and entropies calculated using the property models needed to be converted from molar to specific quantities, molar values were multiplied by associated mixture molar masses, $M_{mix,i}$, evaluated using REFPROP:

$$h_i = h_{m,mix,i} M_{mix,i} \quad (1)$$

$$s_i = s_{m,mix,i} M_{mix,i} \quad (2)$$

State point calculations associated with the compressor are outlined in equations (3) – (11), where the generic functions, $f(*)$, represent the direct or iterative recall of properties from the respective thermodynamic property models. The compressor isentropic efficiency, η_c, was set as a constant for all operating points.

$$h_1 = f(T_1, p_1, \bar{x}_a) \quad (3)$$

$$s_1 = f(T_1, p_1, \bar{x}_a) \quad (4)$$

$$s_{2is} = s_1 \quad (5)$$

$$p_2 = p_1 \times r_c \quad (6)$$

$$T_{2is} = f(s_{2is}, p_2, \bar{x}_a) \quad (7)$$

$$h_{2is} = f(T_{2is}, p_2, \bar{x}_a) \quad (8)$$

$$h_2 = h_1 + \frac{h_{2is} - h_1}{\eta_c} \quad (9)$$

$$T_2 = f(p_2, h_2, \bar{x}_a) \quad (10)$$

$$s_2 = f(T_2, p_2, \bar{x}_a) \quad (11)$$

The specific heat input rate, $\dot{q}_{in}$, and the combustion gas composition, $\bar{x}_g$, were determined for the specified turbine inlet temperature and combustor pressure loss, using thermodynamic properties derived from REFPROP. Assuming complete combustion of the methane fuel, the following adiabatic combustor heat balance is applicable:

$$0 = \sum_{Prod} \dot{n}_{k,3} \Delta h_{k,3} - \sum_{Reac} \dot{n}_{k,2} \Delta h_{k,2} + \dot{q}_r \quad (12)$$

In equation (12), the subscripts $Prod$ and $Reac$ denote the combustion products and reactants, respectively, and $\dot{n}_{k,3}$ and $\dot{n}_{k,2}$ denote the molar flow rate of each species exiting and entering the combustion chamber, respectively. The term Δh_k denotes the enthalpy difference associated with the product and reactant species relative to a reference temperature and pressure of 25 °C and 1 bar, respectively. This quantity was calculated for each product and reactant at the turbine inlet and compressor outlet temperatures, respectively, and at the partial pressure of each species. This rigorous approach required an iterative solution of equation (12), as the mole fractions of the products were initially unknown. The term $\dot{q}_r$ denotes the reaction heat liberation rate and is articulated in equation (13), where $h_{f,k}$ represents the enthalpy of formation of each species.

$$\dot{q}_r = \sum_{Prod} \dot{n}_{k,3} h_{f,k} - \sum_{Reac} \dot{n}_{k,2} h_{f,k,} \quad (13)$$

Enthalpies of formation were obtained from the NIST-JANAF Thermochemical Tables, for a reference temperature and pressure of 25 °C and 1 bar, respectively, as shown in Table 3.

Table 3: Enthalpies of formation for each species.

Species	Enthalpy of Formation (J/mol)
Nitrogen	0
Oxygen	0
Argon	0
Carbon Dioxide	-393522
Water	-241826
Methane	-74873

For an air flow of known composition entering the combustor, the mole rate of each reactant species entering the combustor, $\dot{n}_{k,2}$, can be expressed as a function of the unknown excess air fraction, ε, on the basis of the stoichiometric combustion of methane with oxygen:

$$CH_4 + 2O_2 \longrightarrow CO_2 + 2H_2O \quad (14)$$

$$\dot{n}_{N2,2} = (1 + \varepsilon) x_{N2,2} \quad (15)$$

$$\dot{n}_{O2,2} = (1 + \varepsilon) x_{O2,2} \quad (16)$$

$$\dot{n}_{Ar,2} = (1 + \varepsilon) x_{Ar,2} \quad (17)$$

$$\dot{n}_{CO2,2} = (1 + \varepsilon) x_{CO2,2} \quad (18)$$

$$\dot{n}_{H2O,2} = (1 + \varepsilon) x_{H2O,2} \quad (19)$$

$$\dot{n}_{CH4,2} = 0.5 x_{O2,2} \quad (20)$$

The mole rate of each species produced during combustion can be expressed as a function of the excess air fraction and the composition of air entering the combustor:

$$\dot{n}_{N2,3} = (1 + \varepsilon) x_{N2,2} \quad (21)$$

$$\dot{n}_{O2,3} = (\varepsilon) x_{O2,2} \quad (22)$$

$$\dot{n}_{Ar,3} = (1 + \varepsilon) x_{Ar,2} \quad (23)$$

$$\dot{n}_{CO2,3} = (1 + \epsilon) x_{CO2,2} + 0.5 x_{O2,2} \quad (24)$$

$$\dot{n}_{H2O,3} = (1 + \varepsilon) x_{H2O,2} + x_{O2,2} \quad (25)$$

Once equations (14) – (25) are suitably incorporated, the excess air fraction can be computed iteratively. This allows

the molar rates at the combustor outlet and the combustion gas composition, $\bar{x}_g$, to be determined. The specific heat input rate, $\dot{q}_{in}$, can be evaluated as a function of the excess air fraction, the reaction heat liberation rate, and the molar mass of the air composition, M_a:

$$\dot{q}_{in} = \frac{\dot{q}_r}{(1+\varepsilon)M_a} \quad (26)$$

The above methodology has been validated against combustion calculations performed using the NASA-CEA v2 code in conjunction with suitable data for the lower heating value of methane gas. The state point calculations associated with the turbine are outlined in equations (27) – (39). The turbine isentropic efficiency, η_t, was set as a constant for all operating points.

$$p_3 = p_2(1 - \Delta p_{cc}) \quad (27)$$

$$s_3 = f(T_3, p_3, \bar{x}_{fg}) \quad (28)$$

$$h_3 = f(T_3, s_3, \bar{x}_{fg}) \quad (29)$$

$$s_{4is} = s_3 \quad (30)$$

$$p_4 = p_1 \quad (31)$$

$$T_{4is} = f(s_{4is}, p_4, \bar{x}_{fg}) \quad (32)$$

$$h_{4is} = f(T_{4is}, p_4, \bar{x}_{fg}) \quad (33)$$

$$h_4 = h_3 - \eta_t(h_3 - h_{4is}) \quad (34)$$

$$T_4 = f(p_4, h_4, \bar{x}_{fg}) \quad (35)$$

$$s_4 = f(T_4, p_4, \bar{x}_{fg}) \quad (36)$$

Finally, the cycle performance parameters – specific compressor power input, $\dot{w}_c$, specific turbine power output, $\dot{w}_t$, specific net power output, $\dot{w}_{net}$, and thermal efficiency, η_{th} – were calculated:

$$\dot{w}_c = h_2 - h_1 \quad (37)$$

$$\dot{w}_t = h_3 - h_4 \quad (38)$$

$$\dot{w}_{net} = \dot{w}_t - \dot{w}_c \quad (39)$$

$$\eta_{th} = \frac{\dot{w}_{net}}{\dot{q}_{in}} \quad (40)$$

3 Results and discussion

Deviations associated with the gas turbine performance indices are presented in Figures A1-A5 (Appendix A), relative to predictions by the fixed-composition VDI ideal gas model. The results indicate several noteworthy trends regarding the correlation between models and the sensitivity of performance predictions to parameter variations.

The graphs in Figure A1 show the deviations in the prediction of compressor specific power input as functions of ambient temperature, compression ratio, turbine inlet temperature and ambient relative humidity. A distinctly isolated data spread can be observed in each plot. At the nominal compression ratio of 15, the real gas REFPROP and LibHuFlueGas data sources exhibit an almost constant deviation in the region of 0.25 %, and are in very good agreement. With a variation of compression ratio, the impact of accounting for real gas effects is obvious. At the highest compression ratio of 35 the deviation of the real gas results from the ideal gas reference data exceeds 0.5 %, which is notable. The ideal gas models, even those accounting for dissociation, are all shown to be in very good agreement apart from the model of Lanzafame and Messina, whose data lie significantly offset from the reference data. No sensitivity to the variation of turbine inlet temperature is shown, as this parameter does not influence state point properties associated with the compressor. Sensitivity to changes in ambient relative humidity is shown to be weak.

The graphs in Figure A2 show the deviations in the prediction of turbine specific power output as functions of the ambient and machine parameters. A wider distribution of data is evident in this case, particularly among the ideal gas models. It is believed that this effect is attributable to the compounding of discrepancies during the sequential analysis of the compressor, combustor and turbine. As the compressor outlet temperature influences the combustion analysis, the combustion gas compositions determined by each thermodynamic property model will vary. This variation will in turn be amplified in the turbine analysis. The influence of real gas effects is again indicated by the isolation of the REFPROP and LibHuFlueGas data, and the strong sensitivity of this data to changes in the compression ratio. It is interesting to note however, that the deviation calculated for the latter data is distinctly higher.

This is likely to be as a consequence of the LibHuFlueGas model accounting for dissociation, as this inter-discrepancy is clearly very sensitive to turbine inlet temperature. A significant spread between the dissociation data sets in the turbine inlet temperature graph is also clearly visible, and may be attributable to enhanced real gas effects at high pressure and for working fluids containing greater amounts of water vapour.

The graphs in Figure A3 show the deviations in the prediction of net specific power output as functions of the ambient and machine parameters. Data spread is significant with respect to all independent variables, particularly among the ideal gas data. Once again, a clear distinction between the real and ideal gas data deviations can be seen, as demonstrated by the plots for ambient temperature and ambient relative humidity. The effect of dissociation on net specific power estimations is again indicated by the turbine inlet temperature plot, with strong temperature sensitivity being exhibited as expected. Importantly, for high compression ratios and turbine inlet temperatures, the deviation ranges of approximately 0.5% and 0.75%, respectively, are large. Even at moderate compression ratios and turbine inlet temperatures, the deviation range is still appreciable, and would have significant bearing on gas turbine performance evaluations. Again, wayward predictions are made by the Lanzafame and Messina ideal gas model.

The graphs in Figure A4 show the deviations in the prediction of specific heat input rate as functions of the ambient and machine parameters. For all independent variables the range of deviation is less marked than that associated with the dependent variables considered above; remaining well within a band of 0.25% in each case. Weak sensitivities of the real gas data to compression ratio and turbine inlet temperature are also exhibited, although in either case the deviation between real and ideal gas data decreased at higher combustor pressures and temperatures.

Finally, Figure A5 presents deviations in the prediction of cycle thermal efficiency as functions of the ambient and machine parameters. As in the case of the net specific power output, deviation trends are substantial and widely distributed around the reference ideal gas data. For the variation of compression ratio and turbine inlet temperature, deviation bands are in excess of 0.5%. Again, the Lanzafame and Messina data set displays poor agreement with the other ideal gas data. It can be further observed that there is an increased discrepancy between the deviation trends associated with the REFPROP model, which is a real gas model, and the LibHuFlueGas model, which accounts for both real gas and dissociation effects. This indicates the significance of the impact that dissociation has on the prediction of cycle thermal efficiency, especially for higher turbine inlet temperatures.

The above observations have noteworthy ramifications in regard to the selection of appropriate caloric property models for gas turbine simulations. For high-fidelity simulations where error minimization is of great concern, the results clearly indicate that the selected model should account for both real gas and dissociation effects. This is particularly true in instances where pressures and temperatures exceed approximately 15 bar and 1100 °C, respectively. Beyond these thresholds, deviations between the advanced and ideal gas models for the primary performance indices of net specific power output and thermal efficiency exceed 0.25%.

Figure A6 shows the mean percentage deviations for the key cumulative performance indices of net specific power output and thermal efficiency made by the dissociation models, VDI (D) and NASA-CEA (D), the real gas model, REFPROP, and the dissociation and real gas model, LibHuFlueGas, for variations in the ambient and machine parameters. Inter-comparison of the results presented here offers insight into the significance of accounting for either category of non-ideal effect for the range of parameter variations considered. In this regard, the results appear to indicate that dissociation effects generally have a greater bearing on the overall deviation (as indicated by the LibHuFlueGas data) from the ideal gas approximation than real gas effects, especially in terms of net specific power output. However, the data associated with the variation of compressor pressure ratio show that for a significant range of variation real gas effects are dominant in this case. In an overall sense though, the mean percentage deviation results imply that when model accuracy is a priority, dissociation effects should be captured before real gas effects, although ideally, both effects should be accounted for by the candidate model. In light of these observations, of the models considered here, the LibHuFlueGas model is recommended for use in high-accuracy shaft-power gas turbine simulations.

Where model accuracy is less of a concern or at modest compressor pressure ratios and turbine inlet total temperatures, the ideal gas models appear to be satisfactory for use, apart from the Lanzafame and Messina and McBride *et al.* '93 models, which do not agree well with the remaining ideal gas models. As illustrated in Figure A7, both models under-predict net specific power output and thermal efficiency substantially. The Lanzafame and Messina data shows particularly poor agreement with the reference VDI data. Consistent with the recommendations of ASME[13], the agreement between the VDI and McBride *et al.* '02 models is excellent. It should be noted however, that an advantage of the VDI Guideline 4760 model is that it makes use of only one set of polynomial coefficients and constants for the applicable temperature range, as opposed to the two sets required by the latter model. As such, property computations are made slightly simpler. On the basis of this simplification, the VDI Guideline 4760 model is recommended for use as an ideal gas model for lower-fidelity calculations, or for simulations of cycles characterized by modest peak pressures and temperatures.

What remains to be determined is the importance of accounting for non-ideal effects in the simulation of more complex cycle configurations, such as the regenerative cycle or the reheated cycle. Extrapolating the trends exhibited by the data above, some general predictions can be made in this regard. In regenerative cycles, design compressor pressure ratios are normally kept quite low to optimize thermal efficiency. Turbine inlet total temperatures, however, are not necessarily thermodynamically restricted. As such, it may be anticipated that dissociation effects would contribute most significantly to deviations from the ideal gas approximation. In the case of the reheated cycle, turbine inlet total temperatures are typically high, suggesting that dissociation effects would be significant. Furthermore, since additional fuel is combusted in the exhaust flow leaving the first turbine, secondary combustion gases will contain elevated concentrations of water vapor and carbon dioxide. Subsequently, the impact of real gas effects would be amplified. It is therefore anticipated that for contemporary reheated gas turbines, both dissociation and real gas effects would have a non-negligible influence on thermodynamic properties.

4 Conclusion

This work has assessed the relative correlation between a number of recently-developed and/or commonly-used thermodynamic property data sources in predicting the performance of a shaft-power gas turbine for variations in ambient total temperature, ambient humidity, compression ratio and turbine inlet total temperature. The gas turbine model employed rigorous state point calculations and an adiabatic combustor model, based on real gas property data, to determine the composition of the combustion products in each analysis case, assuming complete combustion of pure methane. The cycle model was used to calculate the compressor specific power input, turbine specific power output, net specific power output, specific heat input rate and thermal efficiency associated with each source of thermodynamic property data.

Results obtained from the analyses indicate a number of noteworthy trends, and suggest that a significant deviation in performance prediction exists amongst the data sources considered. This is particularly true for high compressor pressure ratios and turbine inlet temperatures, where real gas and species dissociation effects become substantial. Predictions derived from the ideal gas models of Lanzafame

and Messina and McBride *et al*. were demonstrated to be in poor agreement with those associated with the VDI reference model. Furthermore, strong sensitivity was indicated for variations in compressor pressure ratio and turbine inlet temperature, with non-ideal gas model data deviating from the reference ideal gas model data by over 0.5% under certain conditions.

It is clear from these observations that for high-accuracy cycle calculations, non-ideal effects should not be neglected – especially considering that data sources accounting for real gas and dissociation effects are today readily available. With this in mind, and in reference to the data sources considered in this work, the FluidEXL Graphics LibHuFlueGas for Excel® thermophysical property software appears to offer the most comprehensive capability and is therefore recommended for use. This is as a consequence of its capacity to account for both real gas and dissociation effects. For lower-fidelity calculations or for cycles characterized by modest peak pressures and temperatures, the application of the state-of-the-art VDI Guideline 4760 ideal gas model would appear to be reasonable.

5 Acknowledgements

The authors wish to acknowledge the financial support provided for this study by the University of KwaZulu-Natal in the form of a Competitive Research Grant.

References

1. *Wagner W, Cooper JR, Dittmann A, Kijima J, Kretzschmar H-J, Kruse A, Mareš R, Oguchi K, Sato H, Stöcker I, Šifner O, Takaishi Y, Tanishita I, Trübenbach J and Willkommen T*. The IAPWS industrial formulation 1997 for the thermodynamic properties of water and steam. *Journal of Engineering for Gas Turbines and Power*, 2000, 122 (1), 150-82.
2. *Bücker D, Span R and Wagner W*. Thermodynamic property models for moist air and combustion gases. J*ournal of Engineering for Gas Turbines and Power*, 2003, 125 (1), 374-84.
3. *Baehr HD and Diederichsen C*. Berechnungsgleichungen für Enthalpie und Entropie der Komponenten von Luft und Verbrennungsgasen. *Brennst.-Wärme-Kraft*, 1988, 40 (12), 30-33.
4. *Brandt F*. Brennstoffe und Verbrennungsrechnung. 2nd ed. Vulkan-Verlag, Essen, 1991.
5. *McBride BJ, Gordon S and Reno MA*. Coefficients for calculating thermodynamic and transport properties of individual species. NASA Technical Memorandum 4513. NASA, Washington, DC, 1993.
6. *Gordon S and McBride BJ*. Computer program for calculation of complex chemical equilibrium compositions and applications. NASA RP-1311. NASA, Washington, DC, 1994.
7. *ANSI/ASME*. Performance test code 4.4 – 1981: Gas turbine heat recovery steam generators. ASME, New York, 1981.
8. *McBride BJ, Zehe MJ and Gordon S*. NASA Glenn coefficients for calculating thermodynamic properties of individual substances. NASA TP 2002-211556. NASA, Washington, DC, 2002.
9. *Lanzafame R and Messina M*. Thermodynamic property models for unburned mixtures and combustion gases. *International Journal of Thermodynamics*, 2006, 9 (2), 73-80.
10. *VDI*. VDI Guideline 4670: Thermodynamic properties of humid air and combustion gases. Verein Deutscher Ingenieure, Berlin, 2003.
11. *Chase Jr MW*. NIST-JANAF thermochemical tables. 4th ed. J. Phys. Chem. Ref. Data 1998, Monograph 9.
12. *SAE*. SAE AS681: Gas turbine engine steady-state and transient performance presentation for digital computer programs. Rev. H., SAE, Warrendale, Pa., 1999.
13. *ASME*. STP-TS-012: Thermophysical properties of working gases used in working gas turbine applications. New York: ASME Standards Technology, LLC, 2008.
14. *Kyprianidis KG, Sethi V, Ogaji SOT, Pilidis P, Singh R and Kalfas AI*. Thermo-fluid modelling for gas turbines – part I: Theoretical foundation and uncertainty analysis. *Proc. ASME Turbo Expo 2009*, Orlando FL, 2009.
15. *Lee AS, Singh R and Probert SD.* Simulations of gas turbine performance: influence of gas-behaviour modeling. *Proceedings of the Institution of Mechanical Engineers, Part A: Journal of Power and Energy*, 2009, 224, 167-77.
16. *Gallar L, Volpe V, Salussolia M, Pachidis V and Jackson, A.* Thermodynamic gas model effect on gas turbine performance simulations. *Journal of Propulsion and Power*, 2012, 28, 719-27.
17. *Kyprianidis KG, Sethi V, Ogaji SOT, Pilidis P, Singh R and Kalfas AI*. Uncertainty in gas turbine thermo-fluid modelling and its impact on performance calculations and emissions predictions at aircraft system level. *Proceedings of the Institution of Mechanical Engineers, Part G: Journal of Aerospace Engineering*, 2012, 226, 163-81.
18. *Lemmon EW, Huber ML and McLinden MO*. NIST reference fluid thermodynamic and transport properties—REFPROP, Version 8.0, User's Guide. Boulder, Co.: NIST, 2007.
19. *Kretzschmar H-J, Stoecker I, Jaehne I, Herrmann S and Kunick M*. Property libraries for working fluids for calculating heat cycles, turbines, heat pumps, and refrigeration processes. *Proceedings of the 2007 ASME International Mechanical Engineering Congress and Exposition*, Seattle WA, 2007.
20. *Gatley DP, Herrmann S and Kretzschmar H*. A Twenty-First Century Molar Mass for Dry Air. HVAC & R Research, 2008, 14 (5), 655-62.

Appendix A

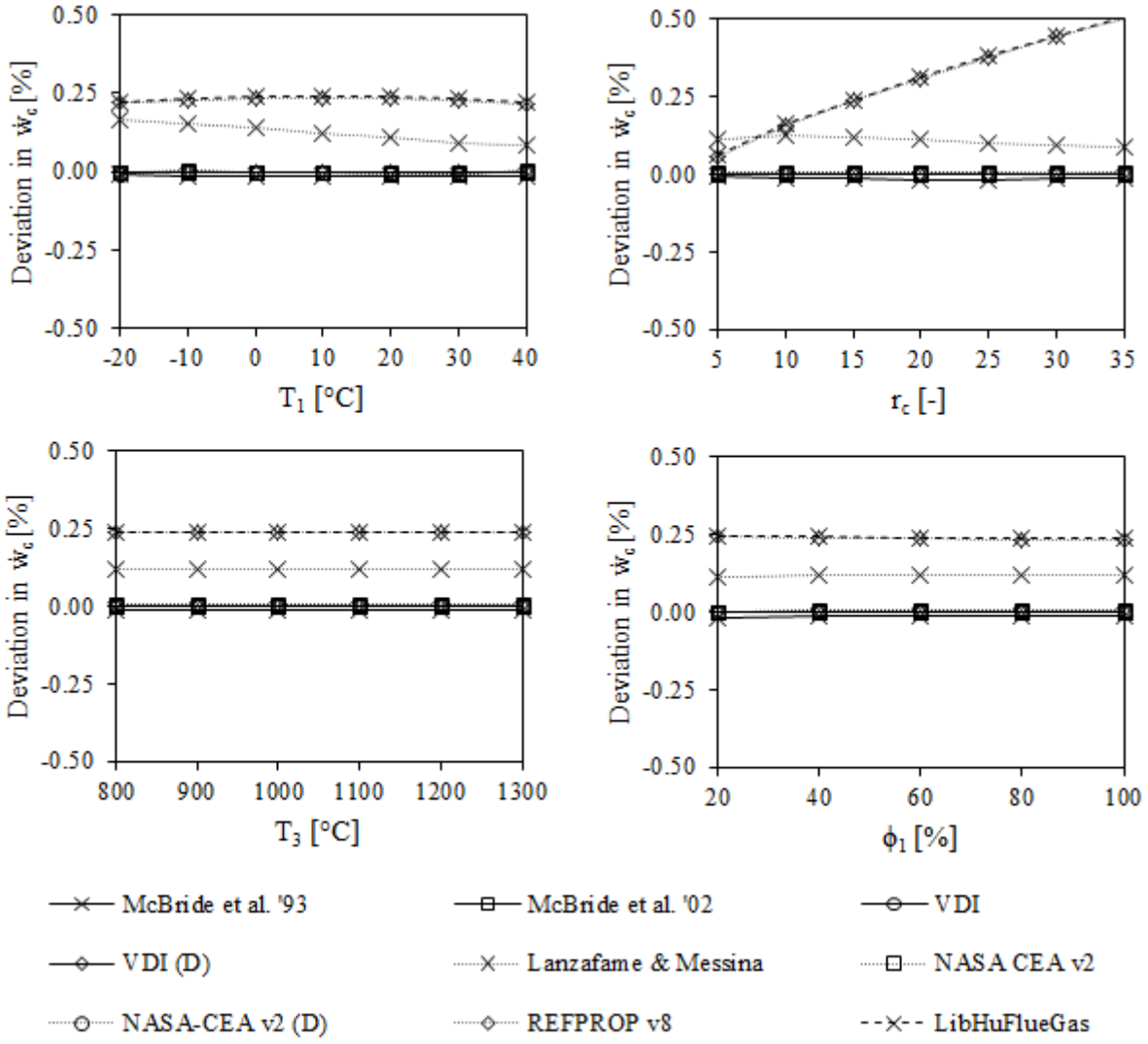

Figure A1: Percentage deviation in compressor specific power input ($\dot{w}_c$) predictions versus ambient temperature (T_1), compression ratio (r_c), turbine inlet temperature (T_3) and ambient relative humidity (ϕ_1).

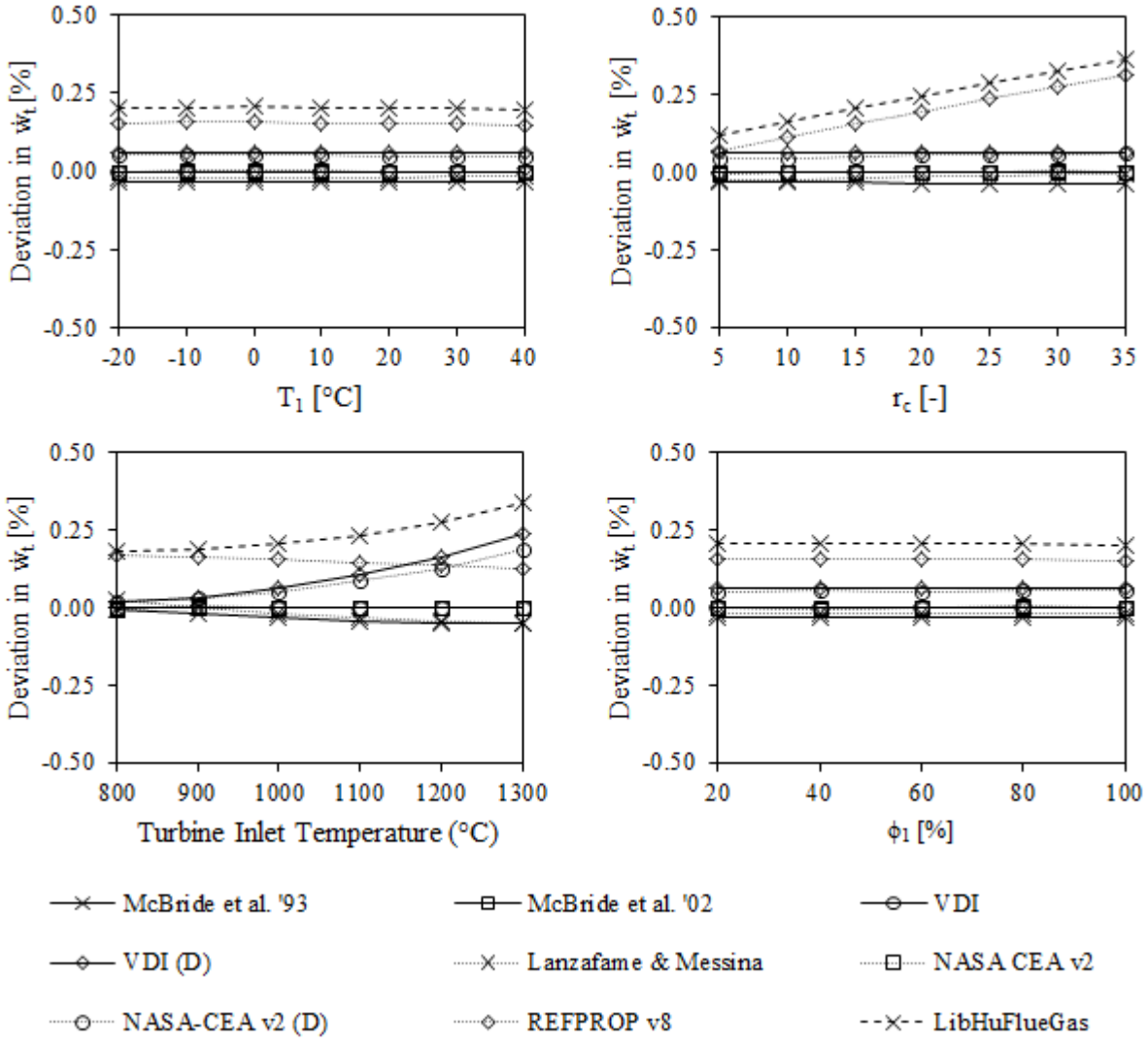

Figure A2: Percentage deviation in turbine specific power output ($\dot{w}_t$) predictions versus ambient temperature (T_1), compression ratio (r_c), turbine inlet temperature (T_3) and ambient relative humidity (ϕ_1).

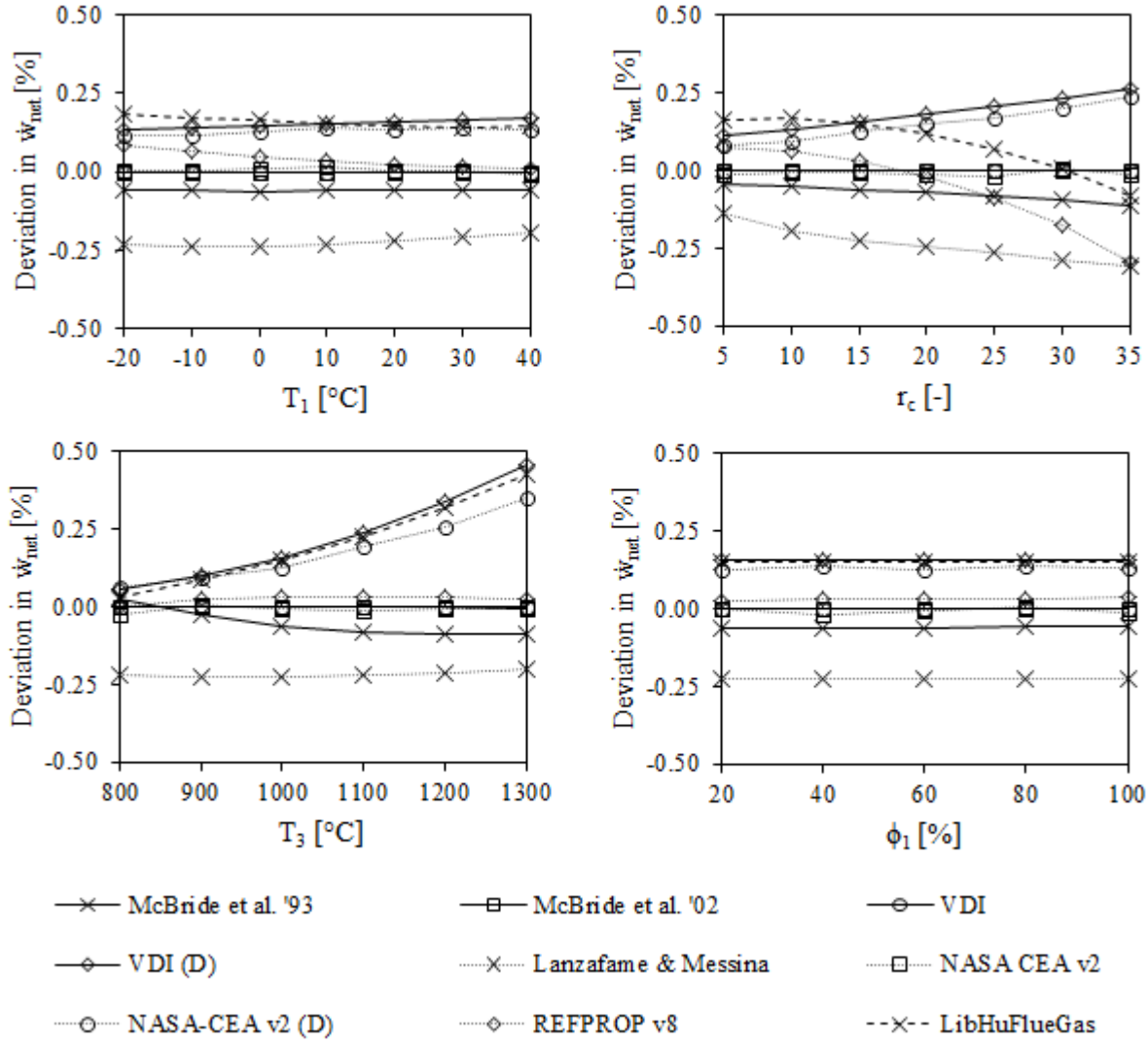

Figure A3: Percentage deviation in net specific power output ($\dot{w}_{net}$) predictions versus ambient temperature (T_1), compression ratio (r_c), turbine inlet temperature (T_3) and ambient relative humidity (ϕ_1).

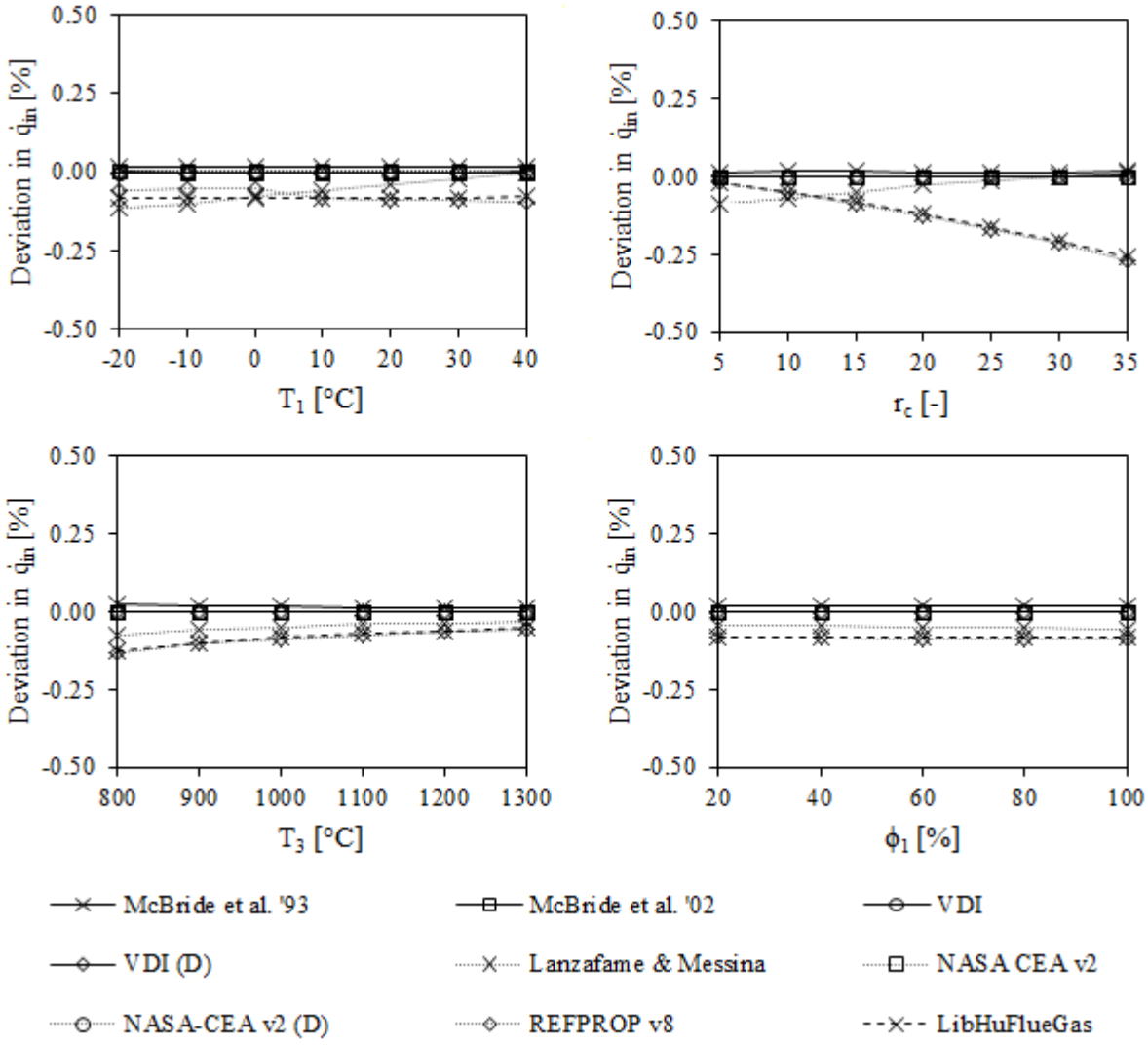

Figure A4: Percentage deviation in specific heat input rate ($\dot{q}_{in}$) predictions versus ambient temperature (T_1), compression ratio (r_c), turbine inlet temperature (T_3) and ambient relative humidity (ϕ_1).

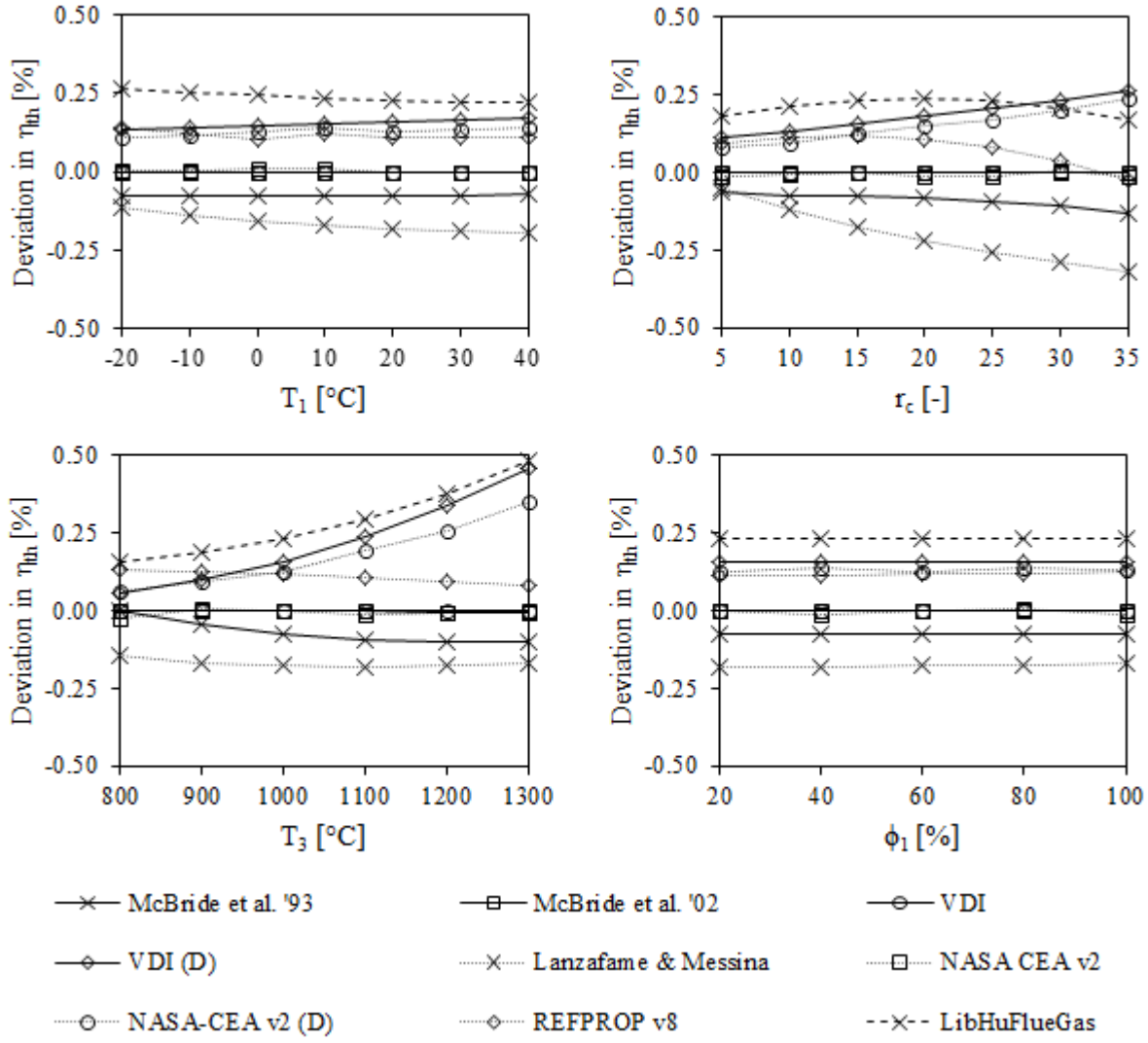

Figure A5: Percentage deviation in thermal efficiency (η_{th}) predictions versus ambient temperature (T_1), compression ratio (r_c), turbine inlet temperature (T_3) and ambient relative humidity (ϕ_1).

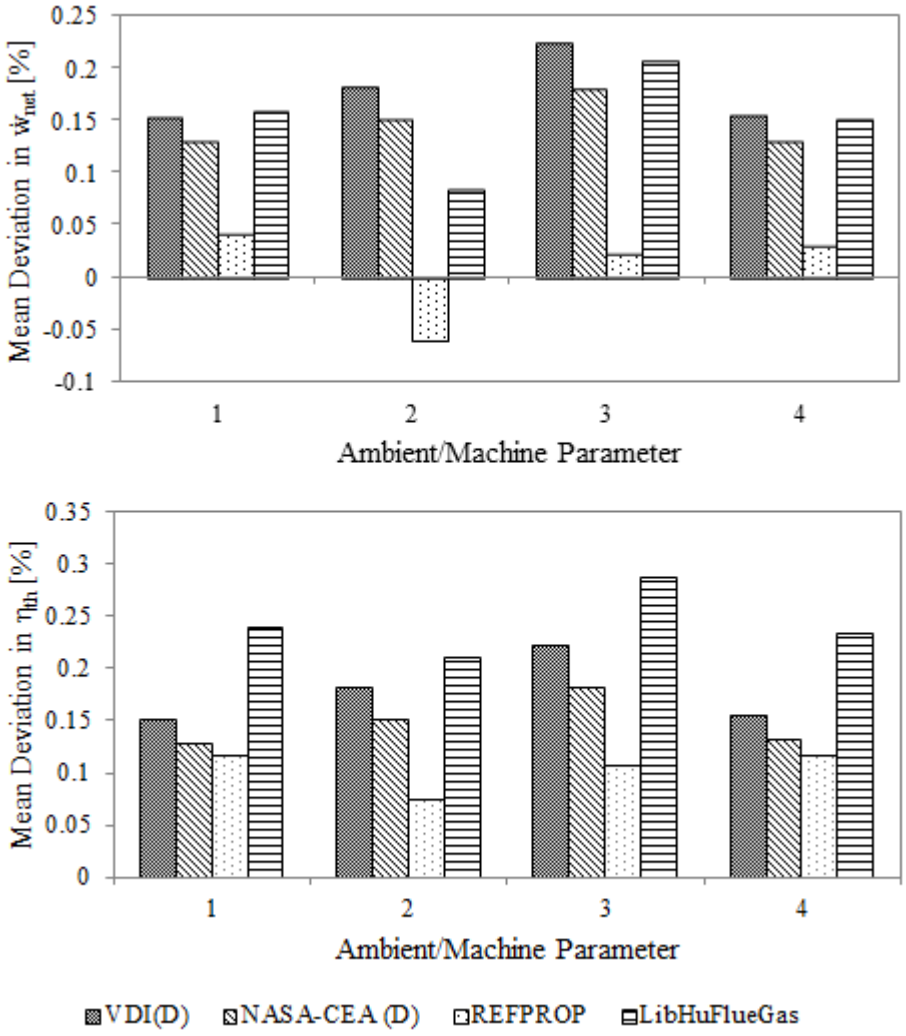

Figure A6: Mean percentage deviations in net specific power output ($\dot{w}_{net}$) and thermal efficiency (η_{th}) predicted by advanced models for variations in 1) compressor inlet temperature, 2) compression ratio, 3) turbine inlet temperature and 4) ambient relative humidity.

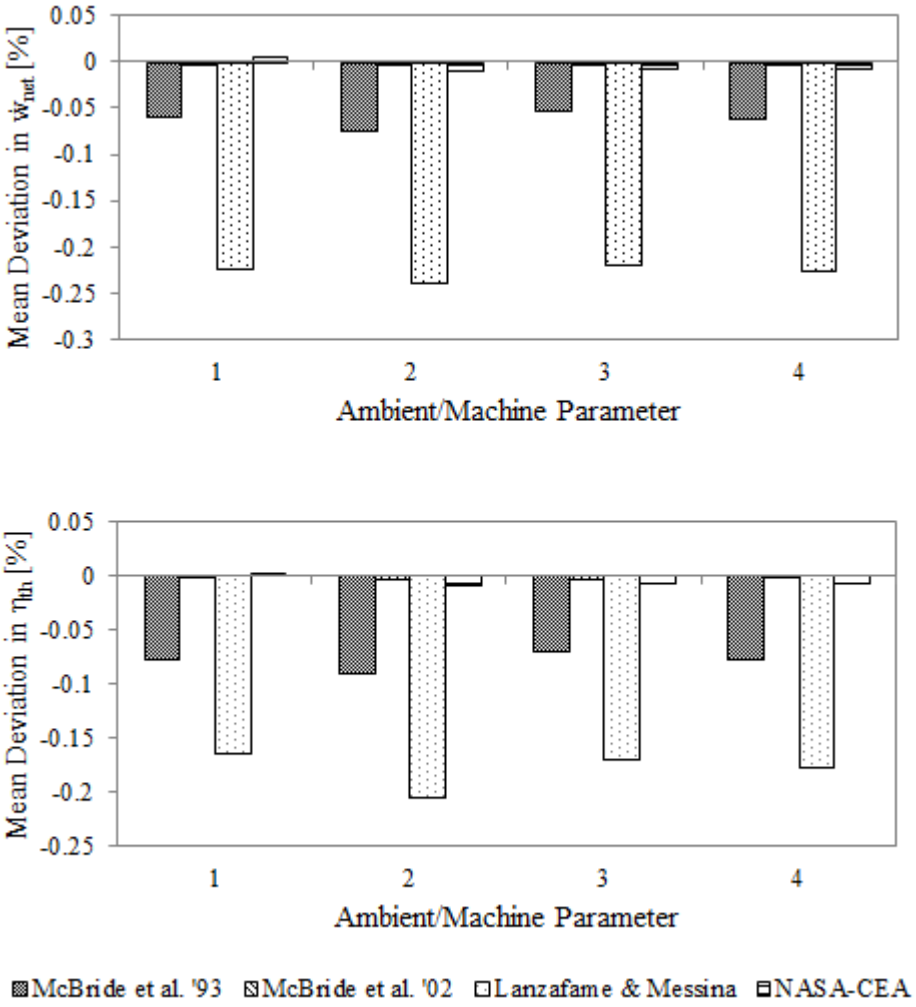

Figure A7: Mean percentage deviations in net specific power output ($\dot{w}_{net}$) and thermal efficiency (η_{th}) predicted by ideal gas models for variations in 1) compressor inlet temperature, 2) compression ratio, 3) turbine inlet temperature and 4) ambient relative humidity.

